DEUTSCHES ELEKTRONEN-SYNCHROTRON DESY

DESY SR 86-06
September 1986

TIME RESOLVED SPECTROSCOPY WITH SYNCHROTRON RADIATION IN THE VACUUM ULTRAVIOLET

by

T. Möller, G. Zimmerer

II. Institut f. Experimentalphysik, Universität Hamburg

ISSN 0723-7979

NOTKESTRASSE 85 · 2 HAMBURG 52

To be sure that your preprints are promptly included in the
HIGH ENERGY PHYSICS INDEX ,
send them to the following address (if possible by air mail) :

DESY
Bibliothek
Notkestrasse 85
2 Hamburg 52
Germany

DESY SR 86-06
September 1986

ISSN 0723-7979

TIME RESOLVED SPECTROSCOPY WITH SYNCHROTRON RADIATION IN THE VACUUM ULTRAVIOLET

by

T. Möller and G. Zimmerer

II. Institut für Experimentalphysik der Universität Hamburg,
Luruper Chaussee 149, D-2000 Hamburg 50,
Fed. Rep. Germany

to be published in Physica Scripta
(Proc. 8th Internat. Conf. on VUV Rad. Physics, Lund (Sweden),
4 - 8 August 1986)

ISSN 0723 - 7979

Abstract

The pulsed nature of synchrotron radiation permits time resolved spectroscopy in the VUV spectral range. In the foreground of discussion is the use of time resolved techniques in fluorescence spectroscopy. The time constants presently accessible extend from the ps to the ms regime, over nearly nine orders of magnitude. The experimental techniques which fit best to the properties of the excitation source, as well as an advanced experimental set-up for time resolved fluorescence spectroscopy, are described. Various results are presented demonstrating the unique possibilities for time resolved VUV spectroscopy offered by synchrotron radiation excitation.

1. Introduction

The outstanding properties of synchrotron radiation (SR) as a light source for spectroscopy in the VUV spectral range are well known and are described in a number of books [1-3]. For the purposes of the present paper we must mention

(i) the tunability over a large spectral range covering the whole VUV part of the electromagnetic spectrum

(ii) the nearly laser-like vertical collimation

(iii) the well defined polarization (100 % linearly polarized within the plane of the orbit, elliptical polarization above and below the plane of the orbit).

The basis of time resolved spectroscopy with SR, however, is

(iv) the pulsed nature of the excitation source.

Since the electrons (or positrons) confined within the storage ring are accelerated only when they are in phase with the radio frequency field produced by the resonant cavities, they are not distributed randomly along their orbit but are collected in so-called bunches. The longitudinal FWHM, l , of the bunches is typically a few cm and the bunches orbit nearly with the speed of light, c. An observer of the radiation emitted from a certain point of the orbit therefore sees flashes of light with a duration $\tau \approx l/c$.

The repetition rate of the radiation pulses is very high. If n bunches are stored, this rate is given by $f = n/T_0 = n\,c/L$ (T_0 is the time per revolution, L is the length of the orbit . In table I, a few representative numerical values of τ, f, etc. are collected.

The potential power of SR excitation for time resolved spectroscopy in the VUV was recognized very early. The pioneering experiments are described by Lindqvist et al. [4] and Heaps et al. [5]. Since then, several reviews were published [6-13]. Different experimental methods of time resolved spectroscopy are well established now, like

(i) real time analysis with single photon counting techniques

(ii) phase fluorometric methods

(iii) time-of-flight methods

(iv) stroboscopic methods.

All of these methods and their applications are described, e.g., in the recent review of Munro and Schwentner[13]. It is not the purpose of the present paper to compete with these reviews but rather to concentrate on those problems in which time resolved spectroscopy with SR permits one to investigate time-dependent phenomena like lifetimes of excited states, intra- and intermolecular dynamics of molecules, energy transfer processes, elementary chemical reactions etc. Of central importance in this context is the field of time resolved fluorescence spectroscopy in the VUV, which will therefore be in the foreground of discussion. The related experimental methods and the considerable progress in instrumentation achieved in the past years are described in sections 2 and 3. In section 4, finally, various experimental results are presented. This paper does not cover those aspects of time resolved spectroscopy in the VUV, which are related to biological problems. This latter topic is presented in a separate paper [14].

2. Experimental methods

2.1 Real time analysis with single photon counting

Real time analysis in connection with single photon counting is an extremely useful and sensitive technique. The essentials are shown

in fig. 1, which includes in the upper part a schematic representation of the time structure of the source with two adjacent excitation pulses separated by $T = T_0/n$.

A single photon event at the photomultiplier PM correlated to excitation pulse (a), is shaped by a discriminator. In order to keep the time jitter due to the pulse height distribution of the PM as small as possible, a constant fraction discriminator (CFD) is often preferred. The shaped pulse starts a time-to-amplitude converter (TAC) which is stopped by a signal synchronized to the excitation pulses. The TAC converts the time interval between "START" and "STOP" to a pulse height. In this particular case it measures $T - \delta$, δ being the time delay between the event at the PM and the corresponding excitation pulse. As shown in fig. 1, a fast preamplifier (PA) is included between the PM and the TAC . This preamplifier is not generally necessary; it's use depends on the amplification of the multiplier used.

The reason why the TAC is started by the event and stopped by the excitation pulse is quite simple. The dead time of the usual electronics is much larger than T. Thus if the TAC were started by the excitation pulse, this would dramatically reduce the sensitivity of the set-up.

Finally, the multichannel analyser (MCA) analyses the height of the TAC pulse. By repeating this procedure again and again, the temporal distribution of the delay, δ , is obtained. This distribution is precisely the time dependent signal created by the excitation pulse. In the simplest case, it is the decay curve of an excited state.

Some restrictions must be taken into consideration.

(i) The counting rate of the PM must be much smaller than the repetition rate (e.g., below 1 % of f). The probability of more than one event per excitation pulse must be negligible, because a second event cannot be detected due to the dead time of the electronics. However, even for the smallest repetition rates available ($f \approx 1$ MHz, see table 1), counting rates up to $\sim 10^4$ cps can be used. Therefore, this is not a severe restriction. Moreover, the use of a pile-up gate would improve the situation considerably.

(ii) The measurement of $T - \delta$ is equivalent to the measurement of δ only if the repetition frequency is very stable. This condition is fulfilled in modern storage rings and allows for a time resolution in the low ps regime.

(iii) The unambiguous assignment of an event to its excitation pulse restricts the duration of the signal to values smaller than T. Only if the signal yields a single exponential decay can lifetimes as long as about ten interpulse periods be accessed [15].

The experimental test of the method is an analysis of the excitation pulse itself. We prefer to measure the so-called apparatus function by monitoring the prompt scattered monochromatic radiation. Such a "stray light spectrum" is shown in fig. 2 [16]. This spectrum was measured with an open channel plate detector sensitized with a coverage of CsI for the near VUV; it represents a convolution of the excitation pulse itself (FWHM = 130 ps) with the response of the detector and the electronics used. To a good approximation the spectral shape is Gaussian. With more conventional multipliers, like the Valvo XP 2020 Q which is widely used in the near VUV and in the UV spectral range, the FWHM is typically about 700 ps.

The FWHM of the apparatus function is a good measure of the ultimate time resolution. A rough estimate of this resolution is a tenth of the measured FWHM of the apparatus function. This means that, under the conditions of [16] (cf. fig. 2), one should be able to measure lifetimes of the order of $\tau \approx 20$ ps $\pm$ 5 ps. The details, however, depend sensitively on the complexity of the signal (i.e., single exponential decay or not), the signal-to-noise ratio etc. The time resolution has been further increased considerably at the storage ring MAX at Lund [14].

The experimental method under discussion allows for a very useful variant (cf. fig. 1). If one includes a single channel (SCA) analyser after the TAC, one can define a time window δt with a delay Δt relative to the excitation pulse. In other words, only those events are allowed to pass through the SCA which occur within the time window δt. With the MCA one can easily visualize the temporal position and width of the time window.

This "gating technique" is not only useful in measuring time resolved fluorescence spectra (examples are given in section 4) but it can also be used to improve the signal-to-dark-count ratio. If the signal is fast (compared with T), it can be measured with an appropriate time window δt without any losses in couting rate. However, the dark counting rate is suppressed by a factor of $\delta t/T$. In this way, it is possible to work at a level of down to 0.1 cps. In other words, the dark counting rate no longer limits the sensitivity. The universal potential power contained in the gating technique may be demonstrated by mentioning an example far outside the scope of the present paper. The pioneering experiment on Mößbauer spectroscopy with SR [17] was only possible because the gating technique allowed for a suppression of the prompt, incoherently scattered x-ray photons against the coherently, time-correlated Mößbauer photons.

2.2 Phase fluorometric methods

The basic idea here has been known for a long time [18]. Suppose that we are given a system with an excited state which emits fluorescence via a single exponential decay. The system may be excited by a sinusoidal, intensity-modulated source

$$I(t) = I_0[1 + \alpha\cos(\omega t)] \tag{1}$$

where α is the modulation amplitude and ω is the angular frequency of the modulation.

The fluorescence signal is the convolution of the excitation function with the decay function $F(t) = \tau^{-1} \exp(-t/\tau)$:

$$A(t) = \int I(t-t')\, F(t')dt' = I_0[1 + \alpha\cos\psi\cos(\omega t - \psi)] \tag{2}$$

The fluorescence signal is therefore modulated with the frequency of the source, but with an attenuated modulation amplitude given by $\alpha\cos\psi$. This signal is phase shifted by an angle ψ, which is defined by

$$\tan\psi = \omega\tau. \tag{3}$$

The modulation ratio m (i.e. the ratio of the two modulation amplitudes) is

$$m = \frac{\alpha\cos\psi}{\alpha} = \cos\psi = (1+\omega^2\tau^2)^{-1/2} \tag{4}$$

Thus a measurement of the phase shift, or of the modulation amplitude, directly yields the lifetime τ of the excited state.

This method can be used with any periodic excitation source. The results for sinusoidal modulation hold for any Fourier component of the excitation and the resultant fluorescence signal [13,19],

$$\tan\psi_n = n\omega_0\tau$$
$$m_n = [1+(n\omega_0\tau)^2]^{-1/2} \tag{5}$$

In these equations n is the number of the Fourier component and $\omega_o = 2\pi f$.

Because of the extremely large disparity between the pulse width and the interpulse period, the intensity of the n th Fourier component is comparable to the intensity at zero frequency (i.e., the average value), even for high n [19]. In other words, the analysis can be performed for high harmonics, still using nearly the entire fluorescence intensity. Therefore, according to eq. (5), very short lifetimes can be measured (down to the sub-ps regime ?) without severe losses in sensitivity.

In the pioneering experiments at SPEAR [20], a direct analysis at about 50 MHz was performed using rf-filters and lock-in techniques. Since a Fourier analysis at some 100 MHz is difficult, a cross-correlation technique was developed, in which the high frequency ($n\,\omega_o$) signal of the detector was mixed with a slightly different frequency ($n\,\omega_o+\Delta\omega$) [19]. The whole information is then deduced from the signal component with the difference frequency $\Delta\omega$. This requires only simple and cheap electronics. Various lifetimes, down to $\tau \approx 500$ ps, were measured with this technique at an accuracy of a few percent [19].

A direct comparison of real time analysis and phase fluorometry with SR has not yet been performed. It is immediately clear that measurements which include the whole Fourier space are equivalent to real time analysis along the full time axis and vice-versa. However, at low fluorescence intensity levels (counting rates below 100 - 1000 cps [19]) the real time analysis seems to be superior at present.

3. The Experimental station SUPERLUMI

In order to illustrate the great utility of time resolved fluorescence spectroscopy, we will now describe an experimental set-up which was designed and successfully implemented over the last several years at HASYLAB.

The beamline and the 2m-NI-monochromator for the spectral selection of the exciting light accept 50 mrad (horizontally) of the SR of a bending magnet [21]. The 'monochromatic' light is focused to a spot in the center of a multipurpose sample chamber. Three different secondary monochromators for the spectral analysis of fluorescence are permanently attached to the sample chamber [22,23]. Numerical parameters of this set-up are given in table II.

The secondary monochromator III covers the spectral range from the near UV to the near IR. The analysis in the VUV spectral range is performed with monochromators I and II. One of these (I) was designed for large acceptance, but aberration limited,medium spectral resolution [22] . This is an f-number 2.8 instrument with extreme sensitivity. If high spectral resolution in a fluorescence spectrum is desired, instrument II, which has a much smaller f-number, can be used [23]. Monochromator II was one of the recent substantial improvements in our set-up. This is demonstrated in fig. 3, which shows a small section of the VUV-fluorescence of the $1\,^1\Sigma_u^+$ state of the Cl_2 molecule [24] excited selectively into a particular vibrational level. The upper curve was measured with monochromator I, the lower curve with monochromator II. In order to improve the signal-to-noise ratio, the gating technique described in sec. 2.1 was used in obtaining the lower curve.

Finally, a recent substantial improvement concerning the dynamical range of time resolution should be mentioned. Because of the high repetition rate of excitation, the accessible long-lifetime limit is in the µs regime even at a big storage ring like DORIS. In order to extend this limit to the ms regime, an ultrafast mechanical chopper was included by Haaks and Kampf [25] between the exit slit of the primary monochromator and the sample chamber. The system is compatible with UHV conditions and uses magnetic bearings, etc. The frequency of rotation can be as high as 1.4 kHz. Fig. 4 shows the dimensions of the chopper disk and a typical time resolved spectrum obtained at the highest frequency. In this way, a really unique dynamical range of time resolution in the VUV extending over nearly nine orders of magnitude is accessible. This can be combined with selective excitation in the VUV and fluorescence analysis over a large spectral range extending from the VUV to the IR.

4. Some selected experimental results

In this section, several examples of time resolved spectroscopy in the VUV with SR excitation are presented. These examples are not chosen randomly but follow an idea which will now be outlined. Time resolved spectroscopy is one of the basic methodologies used to study the properties of excited states of atoms, molecules or solids. The first task, of course, is the determination of the lifetime of an excited state (4.1). Spectroscopy, in general, has also the task to determine the energy of an excited state. Therefore, an example is included in which time resolved methods helped to solve this problem (4.2).

then, of course, time resolved spectroscopy opens the field of excited state dynamics by permitting an analysis of relaxation processes (4.3), energy transfer (4.4), mixing of electronic states (4.5), and investigation of elementary chemical reactions (4.6). (We have to admit, however, that this list is far from exhaustive!)

4.1 Decay curves

In simple systems like, e.g., atoms or molecules at low particle densities, the decay of an excited state can be described by a single exponential, $\exp(-t/\tau)$. An example measured by Schmoranzer et al. [26] is presented in fig. 5. Please note the beautiful exponential decay over more than four orders of magnitude, which stems from the H_2 molecule which was excited selectively into a particular ro-vibronic level. The quantum numbers are given in the figure. It is immediately clear from such data, that lifetimes in the sub-ns regime can be obtained with high accuracy.

4.2 Time resolved fluorescence of a relaxing system and the determination of potential energy curves

This example deals with the determination of excited state potential energy curves of an excimer molecule. Excimers are the subject of several investigations because of their great practical importance as laser molecules for the UV and the VUV spectral range. Rare gas dimers are often regarded as models for excimer molecules. In fig. 6, a set of potential energy curves characteristic of an excimer (realistic for Ar_2) is presented. Note the repulsive ground state, the shallow van der Waals minimum of which cannot be seen in this scale. The molecule possesses two bound excited states terminating

at $^3P_1$ and $^3P_2$ atoms, respectively.

At large internuclear distances, it is possible to determine the excited state potential energy curves from absorption spectroscopy at large particle densities [27] . It is a severe problem, however, to determine the potential energy curves at small internuclear separation. In principle, one has to excite the van der Waals molecules selectively into high vibrational levels of the excited states. This is indicated in fig. 6 by an arrow. Then, one must analyze the spectral distribution of fluorescence, which is of the bound-free type [28]. Especially at the long wavelength onset, one expects to observe an oscillatory behaviour of the emission which stems from the so-called "left" or "inner" turning point region of the molecule. This type of emission directly yields information about the potential energy curves at small internuclear distances.

However, in the past this type of fluorescence spectroscopy was severely impeded by the following problem. A sufficient amount of ground state molecules exists only at high particle densities. Then, as is indicated in the insert in fig. 6, vibrational relaxation competes with radiative decay and in a steady state experiment, even under state selective primary excitation, a superposition of the fluorescence of various vibrational levels is observed. The oscillatory structure is smeared out and the determination of the potential energy curves is strongly hindered.

This problem can be overcome by exploiting the pulsed nature of SR excitation and by using the gating technique described in sec. 2.1. In spite of the vibrational relaxation, it is possible to isolate the fluorescence of the initially excited states (i) if the fluorescence is measured with a time window, the width of which is comparable

to the gas kinetic collision time, and (ii) if the delay to the excitation pulses is zero. Such measurements were performed for the first time at the ACO storage ring [29] . However, the real breakthrough was achieved with the SUPERLUMI station [30] . Fig. 7 presents the fluorescence of the left turning point region of Xe_2, Kr_2 and Ar_2. Clearly, the oscillations are resolved. (It should be noted that the counting rates here were only of the order of 1 % of the counting rates in the maxima of the fluorescence spectra at shorter wavelengths. This is a proof of the extreme sensivity of the set-up using monochromator I for the spectral analysis of fluorescence.)

In fig. 7, the respective excitation wavelengths are given. The long wavelength onset of the bound-free spectrum is clearly correlated with the excitation wavelength, in agreement with theory [30]. Computer simulation of the spectra finally yields the desired information about the excited states (here the 0_u^+ states).

4.3 Time resolved fluorescence spectra and vibrational relaxation

By "time resolved fluorescence spectrum" we mean a fluorescence spectrum (spectral distribution) measured at a given delay to the pulsed excitation. In a practical experiment, the fluorescence is measured within a short time window. Fig. 8 shows such spectra for the Xe_2 molecule [31] . The width of the time window used was 500 ps and 1 ns, respectively. In addition the delay was changed in steps of 500 ps (the delay time is given in the figure). Within the first few ns, the spectral distribution of the fluorescence undergoes dramatic changes as a result of vibrational relaxation of the molecules induced by collisions with Xe atoms. This example was included to demonstrate that in time resolved experiments

under SR excitation it is possible to visualize dynamical changes of the fluorescence distribution even on a sub-ns time scale.

4.4 Relaxation of a matrix-isolated system and energy transfer

In the last years, time resolved spectroscopic methods have come to be more and more used in matrix isolation spectroscopy. As an example, a recent experiment of Kühle et al. [32,33] is discussed. These authors analysed the fluorescence of N_2 molecules in the Xe-matrix, especially that of the A $^3\Sigma_u^+$ state. In a first step, Kühle et al. measured the steady state fluorescence spectra following selective excitation of the N_2 A state (steady state conditions are reached because the lifetime of the emitting state is much longer than the interpulse period of excitation) [32]. From the intensity distribution it was found that the stationary state population of the various vibrational levels of the N_2 A state exhibits a very unusual behaviour. This is shown in the upper part of fig. 9. Besides a schematic potential energy curve for the A state, the population of the vibrational levels is represented by bars. The arrows indicate the initially excited states. The peculiar behaviour could be interpreted in terms of a very interesting type of intermolecular energy transfer correlated with vibrational relaxation due to coupling to the matrix.

It was highly desirable to perform time resolved measurements. After the insertion of the ultrafast mechanical chopper (sec. 3), such measurements became feasible on the SUPERLUMI station [33]. In the lower part of fig. 9, typical decay curves are shown. They qualitatively display the influence of N_2 concentration in the matrix, which is of

crucial importance for the energy transfer process. Whereas at small concentration the decay is more or less of the single exponential type, it clearly becomes non-exponential at higher concentrations. From this dynamical behaviour, details concerning the energy transfer processes can be obtained.

4.5 B/C mixing of rare gas halides (XeCl)

In Cl_2 doped rare gases R (gas phase), it is possible to produce rare gas chlorides in collision processes of the type $R^*+Cl_2 \rightarrow RCl^*+Cl$ or $R+Cl_2^* \rightarrow RCl^*+Cl$ ("*" denotes "electronically excited"). If dynamical aspects of the chlorides are investigated, it is favourable to start with Cl_2^* because the process of formation is very fast. Then, however, selective primary excitation in the VUV spectral range is needed, which is easily performed with SR excitation [34].

The dynamics show up in both the spectral and temporal behaviour of the bound-free fluorescence of the excimers. There exist two adjacent excited states, namely the B (fast radiative decay) and the C (slow radiative decay) state, which are collisionally mixed.

In particular, the decay rates of the B → X fluorescence were analysed [34] as a function of the partial pressures of the gases, in order to obtain information about (i) rate constants of collisional quenching, (ii) energy separation and ordering of the B and C states, and (iii) radiative lifetimes. In fig. 10, the decay rates of the XeCl B → X emission at 308 nm are plotted as a function of the Xe pressure. The Cl_2 pressure was fixed at .8 torr. The open circles were measured at a time, when DORIS was operated with a bunch occupation number n=20 [35], which corresponds

to an interpulse period of only 48 ns. Therefore, measurements at low pressures were not possible. From the open circles, a pressure dependence of the type $K = a + bp + cp^2$ can be deduced. The crosses stem from a study using laser excitation [36] ; except for the high pressure point, there is good agreement with the open circles. Then, however, Inue et al. [37] published results in the low pressure regime (open triangle) which seemed to definitely contradict the prior results. In the meantime, single bunch operation became available at HASYLAB, and the low pressure regime was investigated at the new station SUPERLUMI (full circles) [34] . It turned out that the decay rate indeed showed a peculiar behaviour as is indicated by the full line [34]. The shape of the curve is now understood in detail in terms of a B/C mixing model, with both states being pratically degenerate.

The above result was discussed in some detail because it clearly demonstrates that a large dynamical range in time resolution is indeed required. It is not sufficient to be good in the ps, the ns or even the µs regime. Sometimes it is necessary to control the whole range, which is feasible with the time structure of a big storage ring.

4.6 The first spectroscopic observation of HeH

For the investigation of photochemical reactions, selective excitation of the atoms or molecules involved is highly desirable. With one of the simplest reactions, namely $H_2^* + He \rightarrow$ products, it was demonstrated recently [38] that experiments of this type can be performed with rotational resolution using SR as an excitation source.

As a result of the reaction of excited H_2 molecules with He, the simplest excimer molecule which can exist in nature (and, barring H_2, the simplest molecule of all) is obtained: HeH. For a long time, because of the special interest of theorists in this molecule, quantum mechanical calculations of the potential energy curves were performed [39] . These calculations predicted a strongly repulsive ground state and deeply bound excited states. Even the application of HeH as a laser molecule was discussed before the molecule was observed experimentally [40] .

The first spectroscopic observation of HeH was achieved at the SUPERLUMI station [38] . Fig. 11 presents the fluorescence spectrum of the HeH B (v'=0) state decaying to the repulsive ground state. Without the gating technique to improve the signal-to-noise ratio, this measurement would have hardly been feasible. The broad continuum centered at 240 nm (crosses) is in good agreement with a quantum mechanical calculation of Dohmann et al. [41] . This assignment of the broad emission band to the HeH $B \rightarrow X$ transition was strongly supported by measurements of the lifetime (18 ns), which is in good agreement with theory (19 ns) [41] . In the meantime, HeH has been observed by other groups too [42,43] .

5 Final remarks

It was shown that time resolved spectroscopic techniques in the VUV are accessible now routinely using synchrotron radiation for excitation purposes. This is not only true for atomic and molecular physics, but also for solid state and bio-physics. Many of the expectations expressed in the former articles [4-13] are fulfilled. One of the reasons for the progress achieved in the last years was the development of efficient experimental stations. Another essential condition was the development of fast channel plate detectors which can be combined with several cathode materials. They are therefore sensitive now from the visible to the VUV.

Another big step forward can already be imagined. At serveral places, new dedicated storage rings are under construction or planned. Some of them will offer very sharp excitation pulses (FWHM ~ 10-20 ps) [44]. From the point of view of the source, then 1 ps lifetimes and may be even the sub-ps range will be accessible.

At the same time, the new storage rings are low emittance machines, which are designed for long insertion devices. The next generation of experimental stations for time resolved VUV spectroscopy should be designed in connection with multipole undulators as excitation sources. The photon flux at the exit slit of a primary monochromator may then be an order of magnitude larger than the one of, e.g., the SUPERLUMI station. However, the even more exciting aspect is the tremendous increase of the brilliance of the new sources, which can be used to increase the spectral resolution of excitation in the VUV, may be up to some 10^5. The combination of high spectral and time resolution

with the limits mentioned above seems to be an achievable as well as a worthwhile goal for the developments in the near future.

Acknowledgements

The authors are grateful to the staff of HASYLAB, especially to Dr. P. Gürtler, for the continuous support of the time resolved experiments. The decision of HASYLAB to run DORIS in the four bunch mode during dedicated beamtime was extremely helpful. The enthusiastic efforts of students and co-workers of the University of Hamburg (Dipl.phys. R. Gaethke, Dr. B. Jordan, Dipl.phys. T. Kloiber, Dr. E. Roick, Dipl.phys. J. Stapelfeld) and the fruitful cooperation with colleagues from outside (Drs. M.C. Castex and J. LeCalvé, Paris; Prof. N. Schwentner and Dipl.phys. H. Kühle, Berlin; Prof. D. Haaks and Dipl.phys. S. Kampf, Wuppertal) are gratefully acknowledged. The work was supported by the BMFT of the Federal Republic of Germany.

References

[1] Winick, H. and Doniach, S. (eds.), Synchrotron Radiation Research, Plenum Press New York, 1980

[2] Kunz, C. (ed.), Synchrotron Radiation, Springer-Verlag Berlin Heidelberg New York, 1979

[3] Koch, E.E. (ed.), Handbook on Synchrotron Radiation, Vol. 1A,B, North Holland Amsterdam, 1983

[4] Lindqvist, L., Lopez-Delgado, R., Martin, M.M. and Tramer, A., Proc. of the Internat. Symp. for Synchrotron Radiation Users, Daresbury, Jan. 1973 (eds. G.V. Marr and I.H. Munro), Daresbury Report DNPL/R26, p. 257 (1973)

[5] Heaps, Wm.S., Hamilton, D.S. and Yen, W.M., Opt. Communic. 9, 304 (1973)

[6] Lopez-Delgado, R., Tramer, A. and Munro, I.H., Chem. Phys. 5, 72 (1974)

[7] Lopez-Delgado, R., Course on Synchrotron Radiation Research, Alghero (Italy), 1976, (eds. A.N. Mancini and I.F. Quercia), Vol. I, p. 67. Internat. College of Applied Physics, Catania (Italy), 1976/77

[8] Lopez-Delgado, R., Nucl. Instr. and Meth. 152, 247 (1978)

[9] Monahan, K.M. and Rehn, V., Nucl. Instr. and Meth. 152, 255 (1978)

[10] Hahn, U., Schwentner, N. and Zimmerer, G., Nucl. Instr. and Meth. 152, 261 (1978)

[11] Rehn, V., Nucl. Instr. and Meth. 177, 193 (1980)

[12] Munro, I.H. and Sabersky, A.P. in [1], p. 323

[13] Munro, I.H. and Schwentner, N., Nucl. Instr. and Meth. 208, 819 (1983)

[14] Rigler, R., this volume

[15] Benoist d'Azy, O., Lopez-Delgado, R., and Tramer, A., Chem. Phys. 9, 327 (1975)

[16] Möller, T. and Gürtler, P., Jahresbericht 1985 des Hamburger Synchrotronstrahlungslabor HASYLAB, p. 296, HASYLAB Hamburg, 1985/86

[17] Gerdau, E., Rüffer, R., Winkler, H., Tolksdorf, W. and Klages, C.P., Phys. Rev. Lett. 54, 835 (1985)

[18] Duschinsky, F., Z. Phys. 81, 7 (1933)

[19] Antonangeli, F., Bassani, F., Campolungo, F., Finazzi-Agrò, A., Grassano, U.M., Gratton, E., Jameson, D.M., Piacentini, M., Rosato, N., Savoia, A., Weber, G. and Zema, N., Istitute Nazionale di Fisica Nucleare (Italy), Report LNF-83/68R (1983); Gratton, E., Jameson, D.M., Rosato, N. and Weber, G., Rev. Sci. Instrum. 55, 486 (1984)

[20] Results of K.M. Monahan, I.H. Munro and V. Rehn, publ. in [11]

[21] Wilcke, H., Böhmer, W., Haensel, R. and Schwentner, N., Nucl. Instr. and Meth. 208, 59 (1983)

[22] Gürtler, P., Roick, E., Zimmerer, G., and Pouey, M., Nucl. Instr. and Meth. 208, 835 (1983)

[23] Möller, T., Gürtler, P., Roick, E. and Zimmerer, G., NIMPR A246, 461 (1986)

[24] Results of J. LeCalvé, M.C. Castex, T. Möller, J. Wörner and G. Zimmerer, published in: Möller, T., Kloiber, T. and Zimmerer, G. Jahresbericht 1985 des Hamburger Synchrotronstrahlungslabor HASYLAB, p. 293, HASYLAB Hamburg, 1985/86

[25] Haaks, D. and Kampf, S., Jahresbericht 1985 des Hamburger Synchrotronstrahlungslabor HASYLAB, p. 78, HASYLAB Hamburg, 1985/86

[26] Schmoranzer, H., Imschweiler, J. and Noll, T., Annals of the Israel Phys. Soc. 6, 371 (1983)

[27] Castex, M.C., Spectral Line Shapes, vol. 4, Walter de Gruyter Berlin / New York, 1987 (in press)

[28] Tellinghuisen, J., Photodissociation and Photoionization (ed. K.P. Lawley), p. 299, John Wiley & Sons Ltd. New York, 1985

[29] Dutuit, O., Castex, M.C., LeCalvé, J. and Lavollée, M., J. Chem. Phys. 73, 3107 (1980)

[30] Möller, T., Stapelfeldt, J., Beland, M. and Zimmerer, G., Chem. Phys. Lett. 117, 301 (1985)

[31] Möller, T., Stapelfeldt, J., Beland, M. and Zimmerer, G., unpublished results

[32] Kühle, H., Bahrdt, J.,Fröhling, R., Schwentner, N. and Wilcke, H., Phys. Rev. B31, 4854 (1985)

[33] Kühle, H. and Schwentner, N., Book of Abstracts of VUV8, Lund 1986 (ed. P.O. Nilsson), Vol. I, p. 228, Dept. of Theor. Phys., Lund University, Lund (Sweden), 1986

[34] LeCalvé, J., Castex, M.C., Jordan, B., Zimmerer, G., Möller, T. and Haaks, D., Photophysics and Photochemistry above 6 eV, (ed. F. Lahmani), p. 639, Elsevier Science Publishers B.V. Amsterdam, 1985

[35] Jordan, B., thesis, University of Hamburg, 1983, and Interner Bericht DESY F41 HASYLAB 83-09, September 1983

[36] Grieneisen, H.P., Xue-Jing, H. and Kompa, K.L., Chem. Phys. Lett. 82, 421 (1981)

[37] Inue, G., Ku, J.K. and Setser, D.W., J. Chem. Phys. 80, 6006 (1984)

[38] Möller, T., Beland, M. and Zimmerer, G., Phys. Rev. Lett. 55, 2145 (1985)

[39] Michels, H.H. and Harris, F.E., J. Chem. Phys. 39, 1464 (1963)

[40] Zuev, V.S., Kanaev, A.V. and Mikheev, L.D., Sov. J. Quantum Electron 14, 135 (1984)

[41] Dohmann, H., van Hemert, M. and Peyerimhoff, S.D., to be published

[42] Ketterle, W., Figger, H. and Walther, H., Phys. Rev. Lett. 55, 2941 (1985)

[43] Van der Zande, W.J., Kooi, W., de Bruijn, D.P. and Kubach, C., to be published;
Peterson, J.R. and Bae, Y.K., to be published

[44] A worldwide census of SR facilities has been published by Mühlhaupt, G., NIMPR A246, 845 (1986)

Table I

Selected parameters which are relevant for time resolved spectroscopy in the VUV. Only those storage rings are taken into account, which are in operation. T_o is the orbital period, τ is the FWHM of the pulses, n is the number of bunches and f is the repetition frequency.

Storage ring	T_o(ns)	τ(ns)	n	f(MHz)
SURFII (Washington,USA)	18	1	2	114
SIBERIA-1 (Moscow,USSR)	29	2	1	34,5
SOR-RING (Tokyo,Japan)	57.9	0.7-1.5	1/7	17.3/120.8
ACO (Orsay,France)	72	1.4	1	13.6
TERAS (Ibaraki,Japan)	105	0.5	17	162
MAX (Lund,Sweden)	108	0.05	1/54	9.26/500
VUV (Brookhaven,USA)	170	0.2	1/3	5.88/17.6
UVSOR (Okazaki,Japan)	177	0.3	1/16	5.65/90.4
BESSY (Berlin,W.-Germany)	208	0.07-0.15	1/60/104	4.8/288/500
VEPP-3 (Novosibirsk,USSR)	250	0.6	1	4
ALADDIN (Stoughton,USA)	296	1.2	15	50.7
DCI (Orsay,France)	315		1	3.17
SRS (Daresbury,UK)	320,5	0.05-0.2	1/2/160	3.12/6.24/500
ADONE (Frascati,Italy)	350	0.4	1/18	2.86/51.4
XRAY (Brookhaven,USA)	567	0.3	6	10.58
ALS (Berkeley,USA)	600	0.023	250	417
Photon Factory(Tsukuba, Japan)	624	0.16	312	500
SPEAR (Stanford,USA)	781	0.1 -0.15	4/16	5.12/20.5
DORIS (Hamburg,W.-Germany)	960	0.13	1/4	1.04/4.16
VEPP-4 (Novosibirsk,USSR	1220	0.7		
CHESS (Ithaca,USA)	2560	0.13	3/7	1.17/2.73
PEP (Stanford,USA)	7400	0.05	3	0.405

Table II

Technical parameters of the fluorescence set-up SUPERLUMI

	Resolution interval (nm)	Working range (nm)	Flux/f-number
Excitation			
2m-NI monochromator	$\geq$ 0.007	30 - 300	2×10^{12} photons/s[a]
Fluorescence analysis			
I 0.5 m asymmetric Pouey mounting	$\geq$ 0.5	50 - 300	f/2.8
II 1 m NI monochromator	$\geq$ 0.02	50 - 300	f/10
III 0.5 m (double) monochromator (mod. Czerny-Turner mounting)	$\geq$ 0.03	200 - 1000	f/5

a) This number holds for $\delta\lambda$ = 1 nm at a beam current of 100 mA for a 1200 l/mm grating covered with Al + MgF_2 in the blaze maximum.

Figure captions

Fig. 1 A schematic presentation of the time structure of synchrotron radiation (upper part) and a block diagram of the electronics for real time analysis with single photon counting. (For details see text).

Fig. 2 Temporal analysis of a spectrally resolved VUV DORIS pulse, performed with an open channel plate detector ("stray light spectrum"). The intensity is plotted in a linear and in a logarithmic scale [16] .

Fig. 3 Bound-bound fluorescence of the Cl_2 molecule, which was excited selectively into the $1\,^1\Sigma_u^+$ state with $h\nu$ = 9.16 eV at a gas pressure p = 0.4 torr. The upper curve was measured with monochromator I, the lower curve with monochromator II of the SUPERLUMI station. The resolution intervals $\delta\lambda$ are indicated for each curve [24] .

Fig. 4 Schematic drawing of the chopper disk of SUPERLUMI (upper part) and a decay curve of the Ar_2^* fluorescence at 126.6 nm (Ar pressure = 300 torr, excitation wavelength = 106 nm). The counting rate is given in a logarithmic scale. The dotted line represents the excitation function. (Reproduced from Hanks and Kampf [25] ; by permission of the authors).

Fig. 5 A typical experimental decay curve (dots) of H_2 B , v'=0, J'=1 state at 3.6 mbar, with a least-squares fit (1) of an exponential convoluted with the experimental response function (2). As a result, τ = (535 ± 16) ps was obtained. (Reproduced from Schmoranzer et al. [26] ; by permission of the authors).

Fig. 6 Potential energy curves of an excimer molecule (realistic for Ar_2^*). The $0_g^+ \rightarrow 0_u^+$ excitation and the emission process at the "left turning point" are indicated by arrows, together with a calculated fluorescence spectrum with its oscillatory long wavelength onset [30] . The insert visualizes the superposition of the fluorescence of different vibrational levels coupled by vibrational relaxation.

Fig. 7 Oscillatory long wavelength onset of $0_u^+ \rightarrow 0_g^+$ time resolved fluorescence spectra of Ar_2, Kr_2 and Xe_2. The excitation wavelengths are given in the figure. The gas pressures are 200 torr (Ar) and 100 torr (Kr, Xe). The time windows are 5 ns (Ar), 8 ns (Kr) and 4 ns (Xe) [30].

Fig. 8 Time resolved fluorescence of Xe_2^* at 200 torr. The excitation wavelength is 150 nm. The time window is 500 ps (delay δt = 0) and 1 ns (the other curves). The curve in the background is time integrated [31] .

Fig. 9 Stationary state population of the vibrational levels of N_2 A $^3\Sigma_u^+$ in doped solid Xe (a), and decay curves of the A $^3\Sigma_u^+$ v'=3 level for different N_2 - concentrations (b). For more details see text. (Reproduced from Kühle and Schwentner [33] ; by permission of the authors).

Fig. 10 Decay rate of the B → X emission of XeCl at 308 nm, observed in Xe/Cl_2 mixtures, plotted as a function of the Xe pressure. For more details see text.

Fig. 11 Fluorescence of HeII B $^2\Pi$, v'=0 into the repulsive ground state in He/H_2 mixtures. The excitation wavelength used was 96,5 nm (excitation of H_2 C $^1\Pi_u$, v'=2) [38] . The full curve is the result of a quantum mechanical calculation of Dohmann et al. [41] . (by permission of the authors).

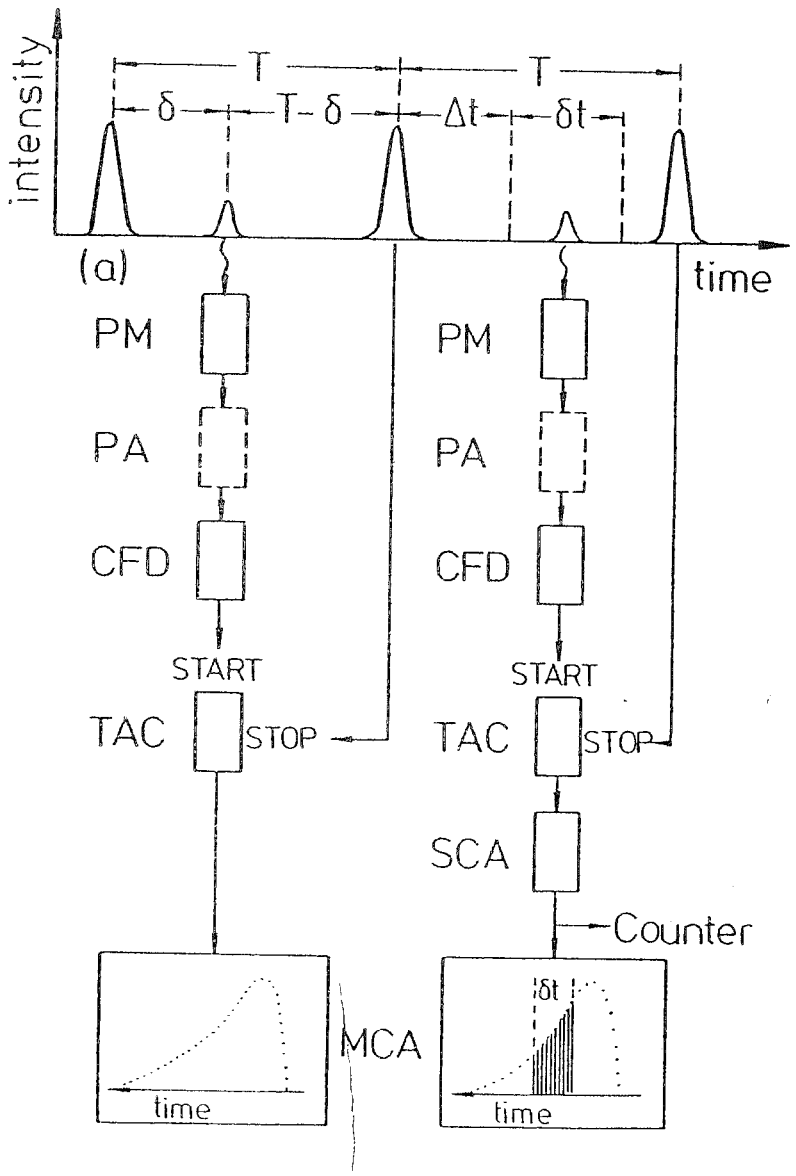

Fig. 1

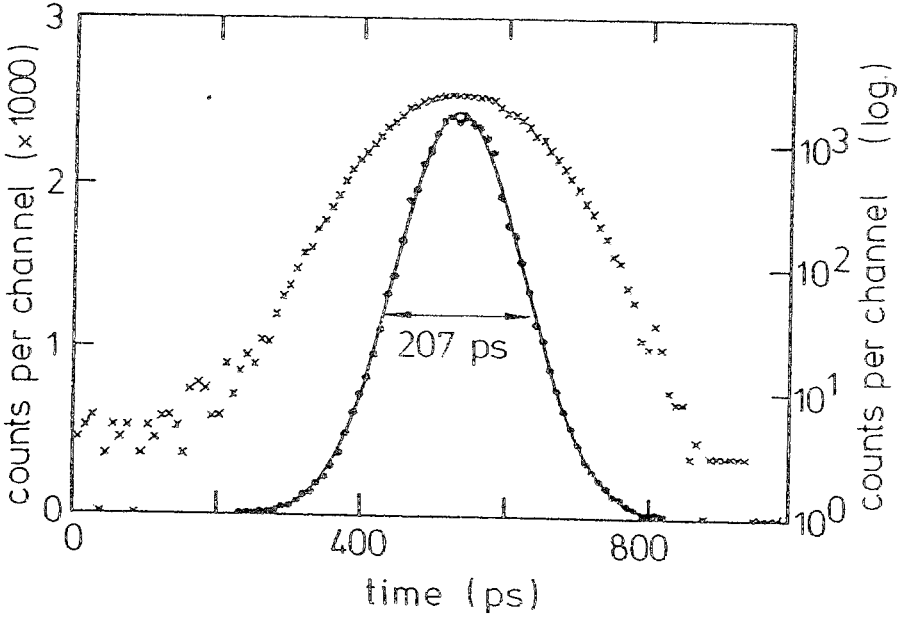
counts per channel (x 1000)
counts per channel (log.)
207 ps
time (ps)
0
400
800
1
2
3
10^0
10^1
10^2
10^3

Fig. 2

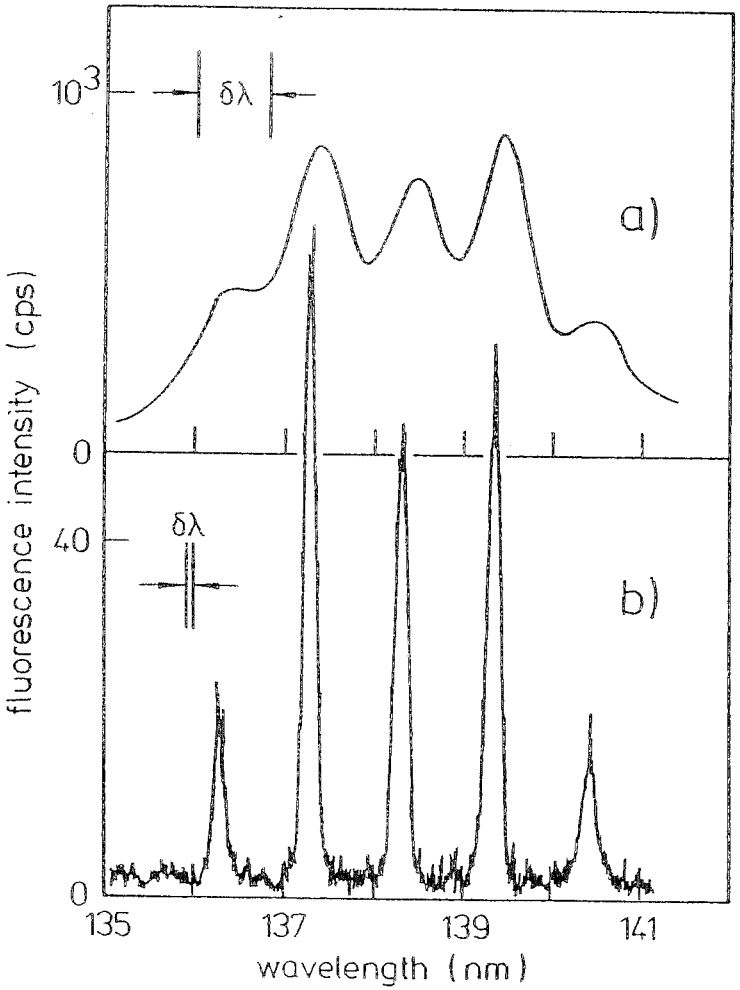
fluorescence intensity (cps)
δλ
a)
δλ
b)
wavelength (nm)
135
137
139
141
0
40
10^3

Fig. 3

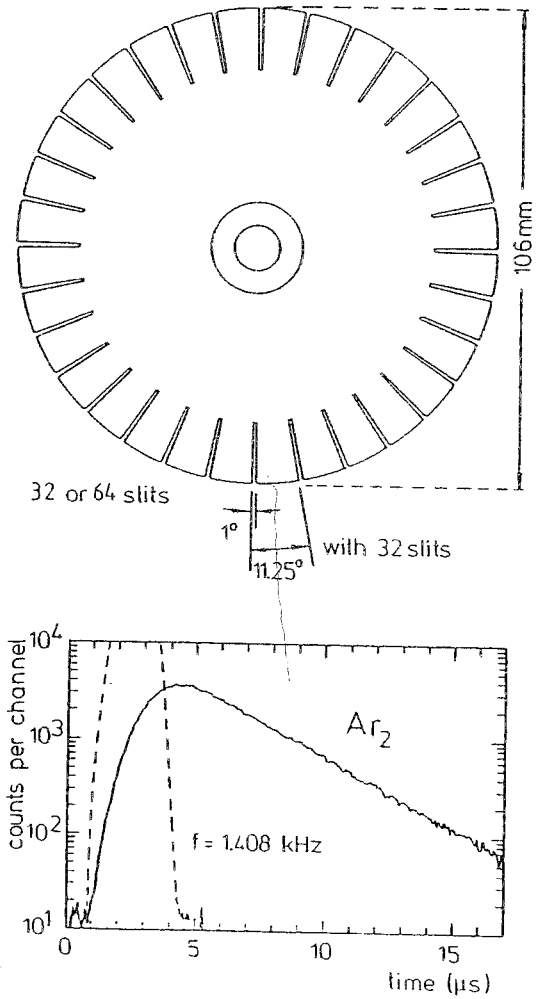
106mm
32 or 64 slits
1°
11.25°
with 32 slits
counts per channel
10^4
10^3
10^2
10^1
Ar_2
f = 1.408 kHz
0
5
10
15
time (μs)

Fig. 4

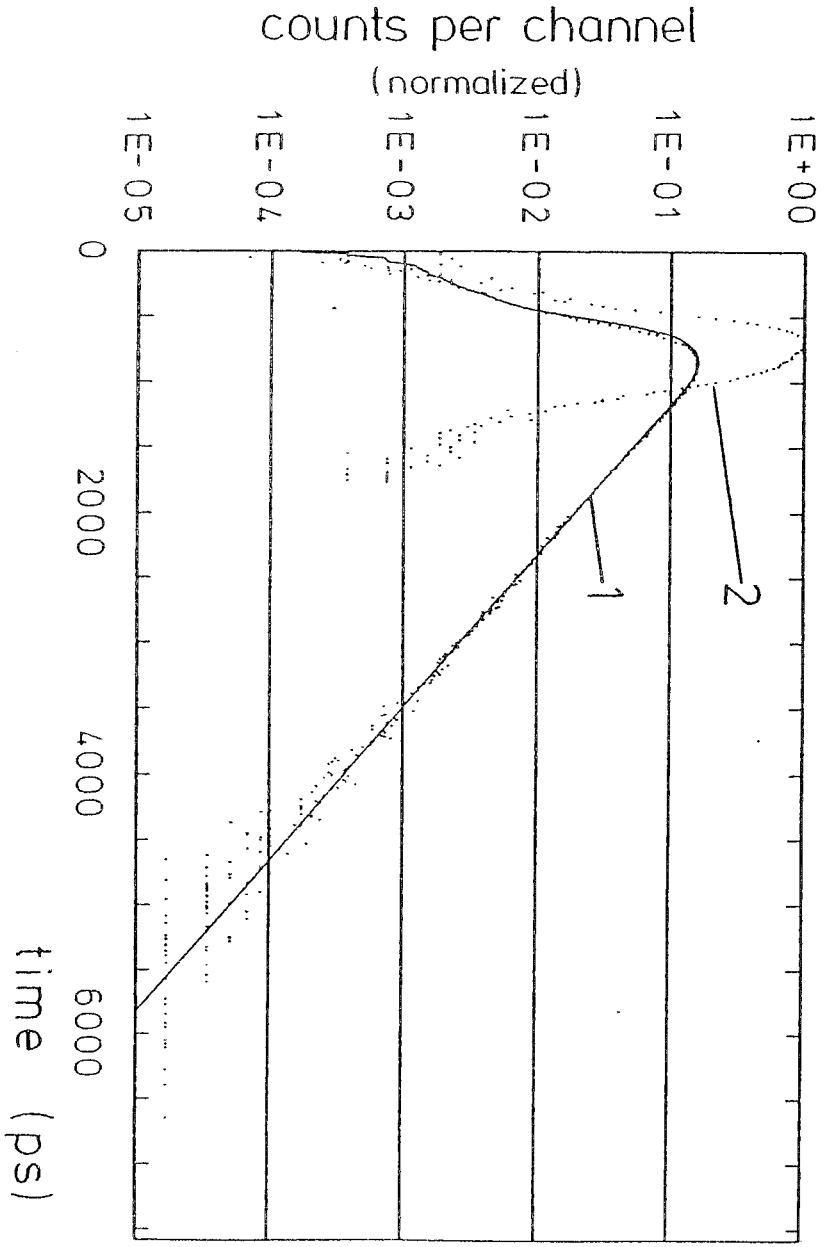
counts per channel
(normalized)
1E-05
1E-04
1E-03
1E-02
1E-01
1E+00
0
2000
4000
6000
time (ps)
1
2

Fig. 5

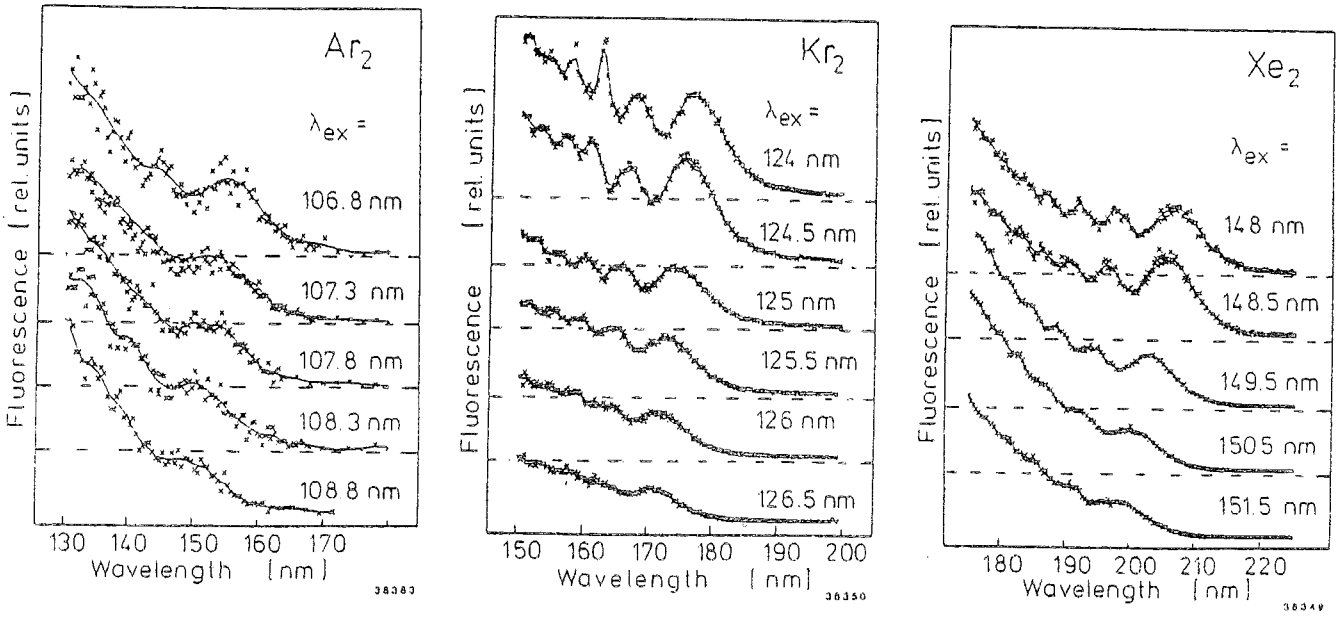
Ar2
λex =
106.8 nm
107.3 nm
107.8 nm
108.3 nm
108.8 nm
Fluorescence [rel. units]
130 140 150 160 170
Wavelength [nm]
Kr2
λex =
124 nm
124.5 nm
125 nm
125.5 nm
126 nm
126.5 nm
Fluorescence [rel. units]
150 160 170 180 190 200
Wavelength [nm]
Xe2
λex =
148 nm
148.5 nm
149.5 nm
150.5 nm
151.5 nm
Fluorescence [rel. units]
180 190 200 210 220
Wavelength [nm]

Fig. 7

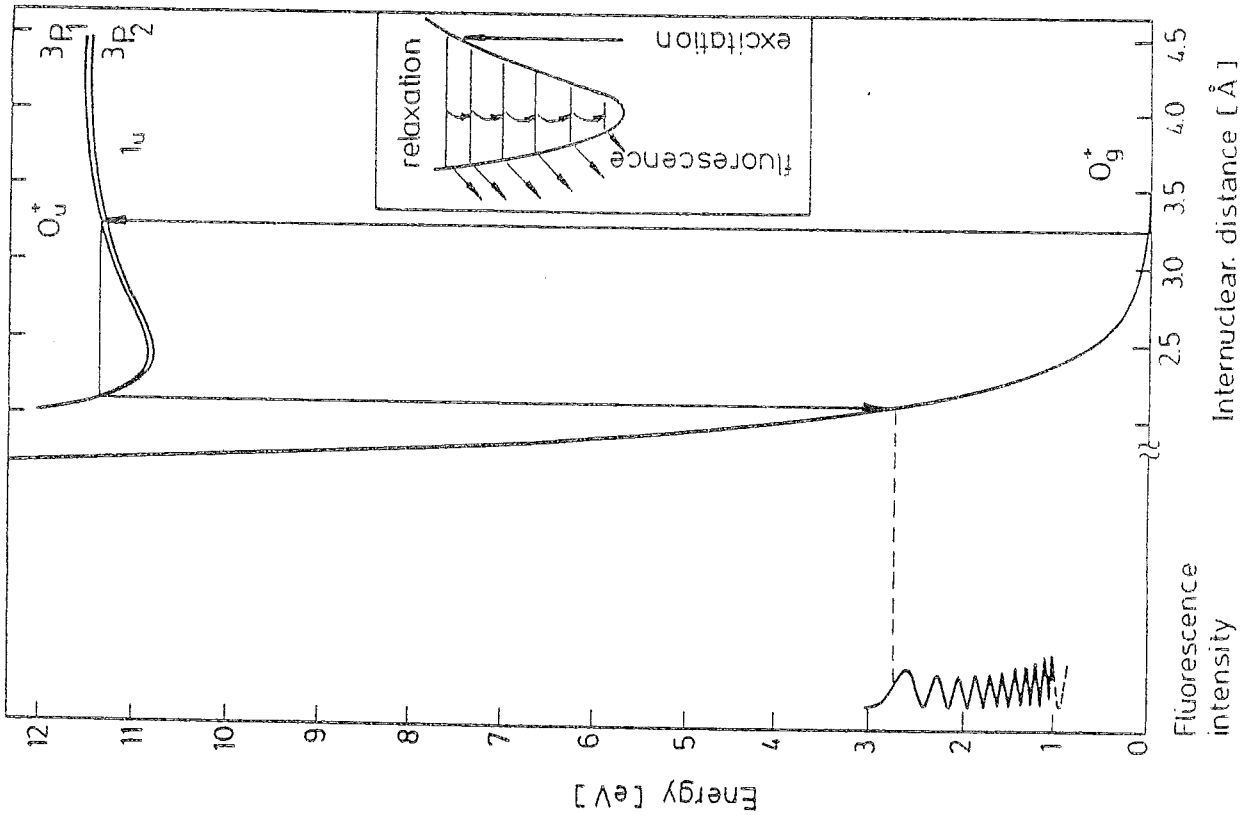
3P1
3P2
1u
O+u
O+g
relaxation
excitation
fluorescence
Internuclear distance [Å]
2.5 3.0 3.5 4.0 4.5
Fluorescence intensity
Energy [eV]
12 11 10 9 8 7 6 5 4 3 2 1 0

Fig. 6

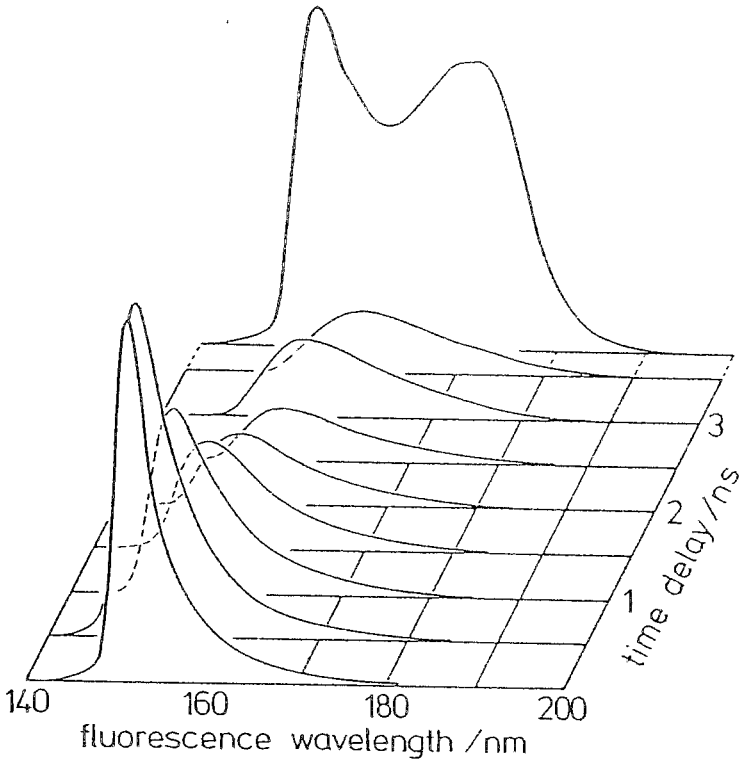
140
160
180
200
fluorescence wavelength /nm
1
2
3
time delay/ns

Fig. 8

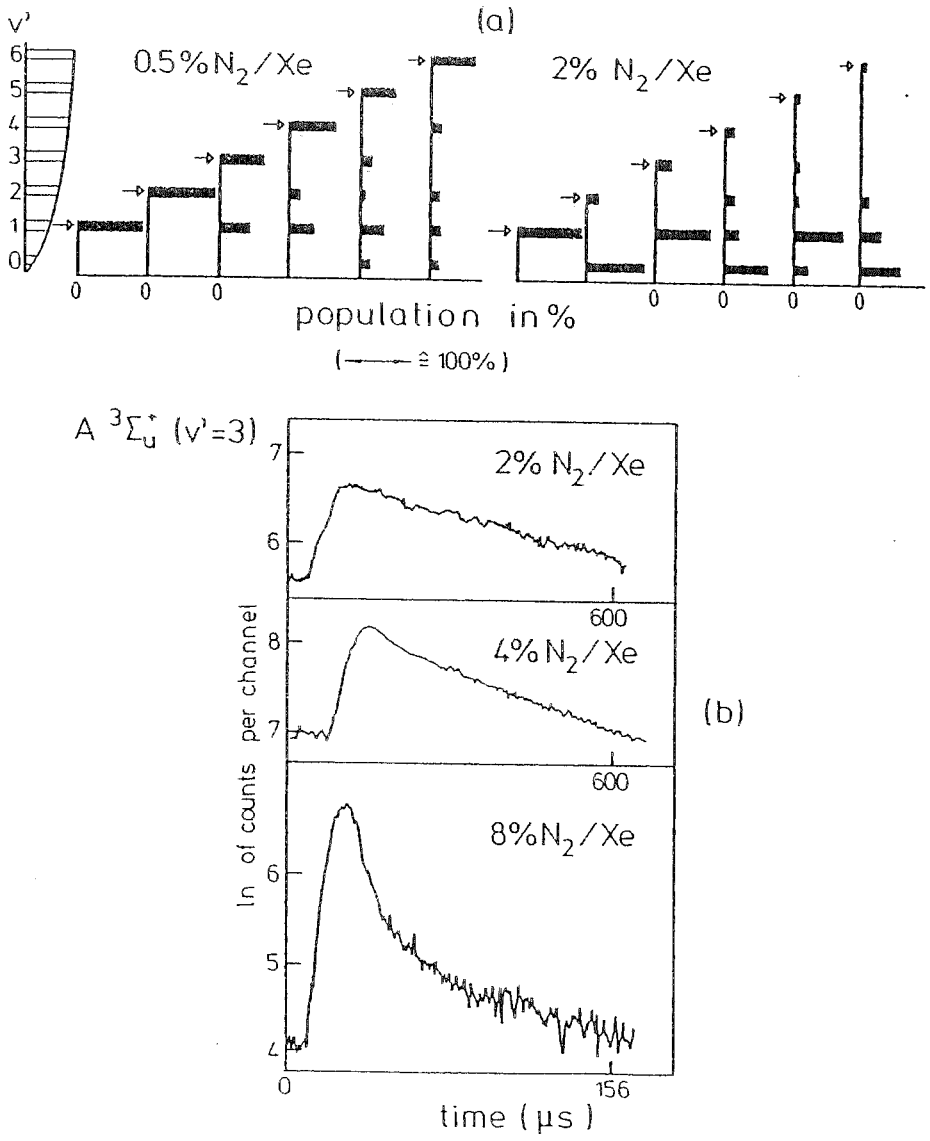
(a)
v'
6
5
4
3
2
1
0
0.5% N_2/Xe
2% N_2/Xe
0 0 0
0 0 0 0
population in %
(—— ≙ 100%)
A $^3\Sigma_u^+$ (v'=3)
2% N_2/Xe
4% N_2/Xe
8% N_2/Xe
600
600
156
ln of counts per channel
time (μs)
(b)

Fig. 9

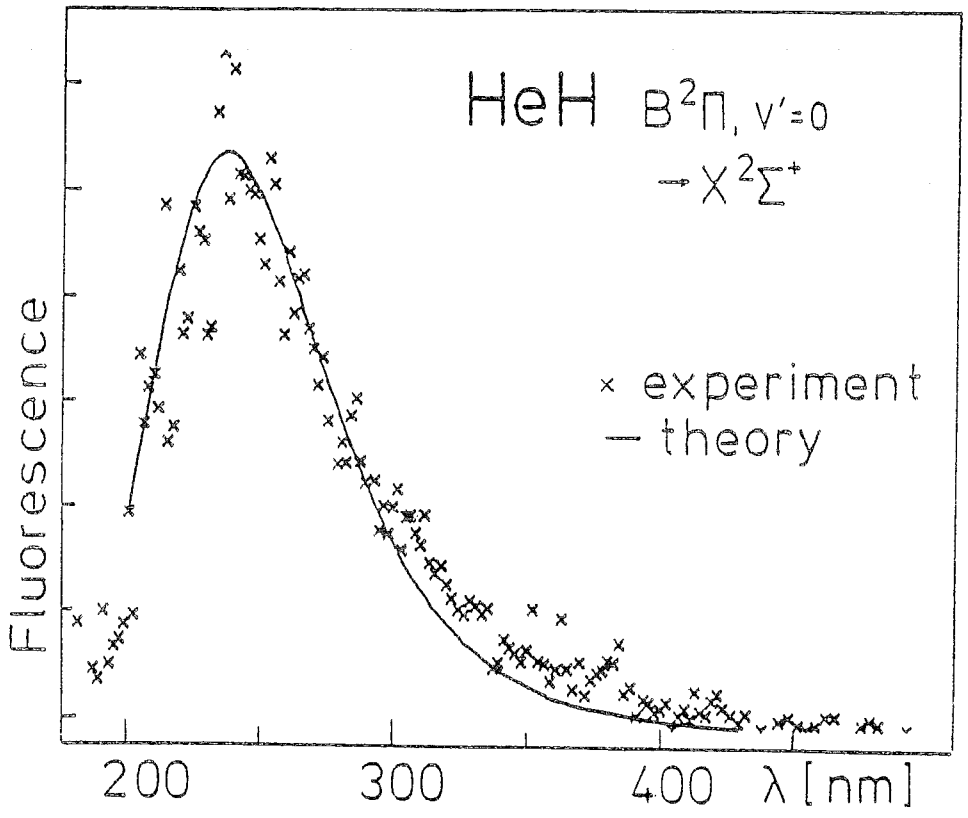
HeH $B^2\Pi$, v'=0
$\rightarrow X^2\Sigma^+$
× experiment
— theory
Fluorescence
200
300
400
λ [nm]

Fig. 11

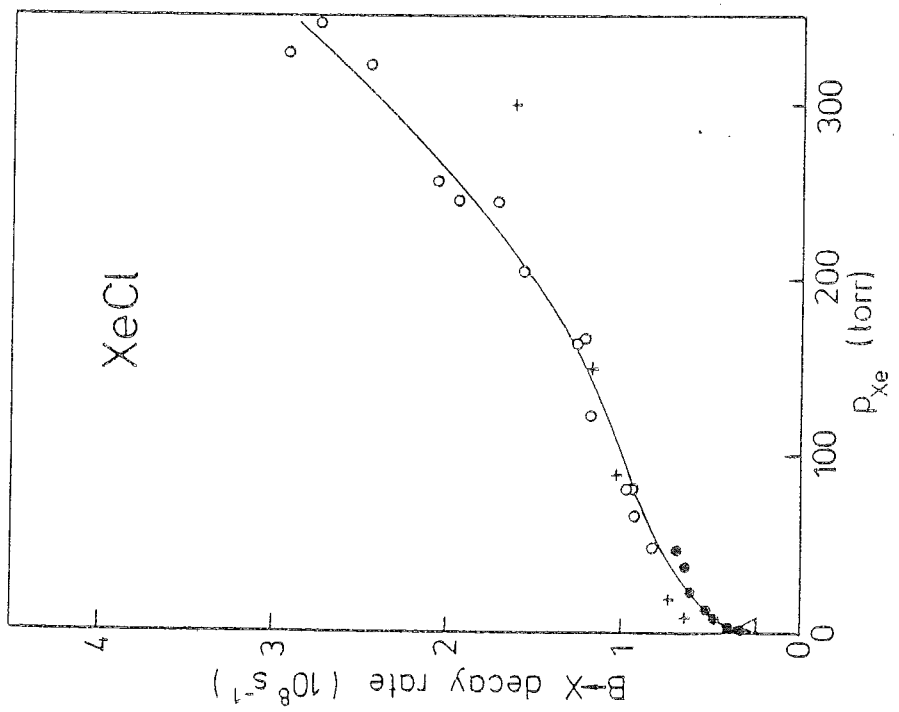
XeCl
B→X decay rate (10^8 s^{-1})
0
1
2
3
4
0
100
200
300
P_{Xe} (torr)

Fig. 10